

# KECK DEEP FIELDS. III. LUMINOSITY-DEPENDENT EVOLUTION OF THE ULTRAVIOLET LUMINOSITY AND STAR FORMATION RATE DENSITIES AT $z\sim 4, 3$ , AND 2<sup>1</sup>

MARCIN SAWICKI

Department of Physics, University of California, Santa Barbara, CA 93106, USA; and Dominion Astrophysical Observatory, Herzberg Institute of Astrophysics, National Research Council, 5071 West Saanich Road, Victoria, B.C., V9E 2E7, Canada

DAVID THOMPSON

Large Binocular Telescope Observatory, University of Arizona, 933 N. Cherry Ave., Tucson, AZ 85721-0065, USA; and Caltech Optical Observatories, California Institute of Technology, MS 320-47, Pasadena, CA 91125, USA

*Accepted for publication in the Astrophysical Journal*

## ABSTRACT

We use our very deep Keck Deep Fields  $U_nGRI$  catalog of  $z\sim 4, 3$ , and 2 UV-selected star-forming galaxies to study the evolution of the rest-frame 1700Å luminosity density at high redshift — a study that is motivated by our finding of luminosity-dependent evolution of the galaxy luminosity function at high redshift. Ours is the most robust UV luminosity density measurement to date at these redshifts as it uses a well-tested object selection technique, several independent sightlines, and probes deep into the galaxy luminosity function. The ability to reliably constrain the contribution of faint galaxies is critical and our data do so as they reach deep into the galaxy population, to  $M_{L_{BG}}^*+2$  even at  $z\sim 4$  and deeper still at lower redshifts (where  $M_{L_{BG}}^*=-21.0$  is the Schechter function's characteristic magnitude for Lyman break galaxies (LBGs) and  $L_{L_{BG}}^*$  is the corresponding luminosity). We find that the luminosity density at high redshift is dominated by the hitherto poorly studied galaxies fainter than  $L_{L_{BG}}^*$ , and, indeed, the bulk of the UV light in the high- $z$  Universe comes from galaxies in the rather narrow luminosity range  $L=0.1-1L_{L_{BG}}^*$ . It is these faint galaxies that govern the behavior of the total UV luminosity density. Overall, there is a gradual rise in luminosity density starting at  $z\sim 4$  or earlier (we find twice as much UV light at  $z\sim 3$  as at  $z\sim 4$ ), followed by a shallow peak or a plateau within  $z\sim 3-1$ , and then followed by the well-know plunge at lower redshifts. Within this total picture, luminosity density in sub- $L_{L_{BG}}^*$  galaxies evolves more rapidly at high redshift,  $z\gtrsim 2$ , than that in more luminous objects. However, this is reversed at lower redshifts,  $z\lesssim 1$ , a reversal that is reminiscent of galaxy downsizing, albeit here thus far seen only in galaxy luminosity and not yet in galaxy mass. Within the context of the models commonly used in the observational literature, there seemingly aren't enough faint or bright LBGs to maintain ionization of intergalactic gas even as late as  $z\sim 4$ . This is particularly true at earlier epochs and even more so if the faint-end evolutionary trends we observe at  $z\sim 3$  and 4 continue to higher redshifts. Apparently the Universe must be easier to reionize than some recent studies have assumed. Nevertheless, sub- $L_{L_{BG}}^*$  galaxies do dominate the total UV luminosity density at  $z\gtrsim 2$  and this dominance further highlights the need for follow-up studies that will teach us more about these very numerous but thus far largely unexplored systems.

*Subject headings:* galaxies: evolution — galaxies: formation — galaxies: high-redshift — galaxies: starburst

## 1. INTRODUCTION

The global, volume-averaged UV luminosity density of the Universe, and the global star formation rate density that is often derived from it, contain important information regarding the formation and evolution of galaxies, the populating of the Universe with stars, and the production of heavy elements in the cosmological context.

The first measurement of the time evolution of the cosmic UV luminosity density was done by Lilly et al. (1996) who found a remarkable drop in the luminosity density over the redshift interval from  $z\sim 1$  to  $z\sim 0$  which, with the help of stellar population synthesis models, they in-

terpreted as an order-of-magnitude decline in cosmic star formation rate since  $z\sim 1$ . The public release of Hubble Deep Field data soon thereafter (HDF; Williams et al. 1996) made it possible to extend such studies to higher redshifts,  $z\sim 1-4$ , and in nearly concurrent work (the two papers were published only a month apart) Madau et al. (1996) placed lower limits<sup>2</sup> on the star formation rate density at  $z\sim 3$  and 4, while Sawicki, Lin, & Yee (1997) estimated the UV luminosity density in  $M_{UV}(AB)>-15$  galaxies over  $z\sim 1.5-3.5$ , and concluded that the onset of star formation in the Universe occurred at  $z>3.5$ .

Much subsequent work has focused on either extending the analysis to higher redshifts (e.g., Lehnert & Bremer 2003; Bunker et al. 2004; Yan et al. 2004; Bouwens et al. 2006) in attempts to identify the galaxy population responsible for cosmic reionization, or on assessing the

<sup>2</sup> The Madau et al. (1996) analysis included neither incompleteness corrections nor a uniform limiting magnitude.

Electronic address: sawicki@physics.ucsb.edu  
Electronic address: dthompson@as.arizona.edu

<sup>1</sup> Based on data obtained at the W.M. Keck Observatory, which is operated as a scientific partnership among the California Institute of Technology, the University of California, and NASA, and was made possible by the generous financial support of the W.M. Keck Foundation.

corrections for dust either by measuring attenuation in optically-selected galaxies (e.g., Sawicki & Yee 1998; Papovich et al. 2001; Shapley et al. 2001; Reddy & Steidel 2004; Iwata, Inoue, & Burgarella 2005a), tracking down the contribution of rare but vigorously star-forming sub-millimeter-selected galaxies (e.g., Smail et al. 1997; Barger et al. 1998; Eales et al. 1999; Chapman et al. 2005; Sawicki & Webb 2005), or attempting to relate these two star-forming populations (e.g., Chapman et al. 2000; Sawicki 2001; Baker et al. 2001; Webb et al. 2003).

However, the early HDF-based results (e.g., Madau et al. 1996, 1998; Sawicki et al. 1997; Connolly et al. 1997) on which the picture at  $z\sim 1-4$  was based suffered from a serious drawback: they were based on a single, tiny field and thus subject to both Poisson noise and potential systematic problems related to large-scale structure effects (often referred to as “cosmic variance”). Recognizing this as a serious problem, Steidel et al. (1999) used their large, spectroscopically-calibrated and multi-field Lyman break galaxy samples to constrain the UV luminosity function and cosmic star formation rate density at  $z\sim 3$  and 4. Their conclusion was that there was no evidence for evolution in either the galaxy luminosity function or cosmic SFR density from  $z\sim 3$  to  $z\sim 4$ . However, the Steidel et al. ground-based surveys contain only galaxies brighter than  $M^*+1$  at  $z\sim 3$  and  $M^*$  at  $z\sim 4$ . Consequently, while the bright end of the galaxy population in their study is reasonably well constrained, these authors, too, had to rely on HDF data to measure the LF below  $\sim L^*$ . Specifically, at  $z\sim 3$  they used the HDF LBG counts to constrain the LF’s faint end, reporting it to be  $\alpha = -1.6$ ; however, lacking sufficient statistics for faint  $z\sim 4$  galaxies in the HDF they were then forced to *assume* the same  $\alpha = -1.6$  faint end slope for their  $z\sim 4$  measurement. Thus, the Steidel et al. (1999)  $z\sim 3$  luminosity density measurement is in fact highly reliant on the single tiny HDF, while their  $z\sim 4$  luminosity density measurement, and the conclusion that the SFR density does not evolve between  $z\sim 4$  and  $z\sim 3$  is based on the *assumption* of a non-evolving faint end of the LF.

Meanwhile, the contribution of faint, sub- $L^*$  galaxies to the cosmic luminosity density and star formation rate cannot be stressed strongly enough. As Fig. 1 illustrates, for most reasonable luminosity functions it is exactly the faint, hitherto poorly constrained sub- $L^*$  galaxies that produce the bulk of the total light. The Steidel et al. (1999, 2003) ground-based surveys are so shallow that they capture only about a third of the total light at  $z\sim 3$  and less than  $\sim 20\%$  at  $z\sim 4$  and similar limitations apply to much of the recent work at higher redshifts. The inference about the remaining yet dominant bulk of the UV luminosity density is based on poorly-constrained HDF-based extrapolations to fainter luminosities.

Recognizing the limitations of the Steidel et al. (1999, 2003, 2004) surveys, we have recently undertaken an imaging survey specifically targeting intrinsically faint, sub- $L^*$  Lyman break galaxies. Our survey, the Keck Deep Fields (KDF; Sawicki & Thompson 2005, 2006) selects  $z\sim 4$ , 3, and 2 galaxies using the *very same*  $U_nGRI$  filter set and color-color selection criteria as those used by the Steidel team and, indeed, our photometry is even further calibrated onto that of Steidel et al. since some of our KDF fields are co-located with theirs. This approach gives us a uniquely well-defined, characterized,

and robust sample, but one that probes 1.5 magnitudes deeper than the Steidel et al. work and so reaches significantly below  $L^*$ : even at  $z\sim 4$  we reach  $M^*+2$  and so can constrain the shape of the all-important faint end of the luminosity function very well.

Using these very deep KDF data, we found a shallower LF faint-end slope at  $z\sim 3$  than did Steidel et al. (1999):  $\alpha = -1.43$  vs. their HDF-based  $\alpha = -1.6$ ; and an even shallower one at  $z\sim 4$ :  $\alpha = -1.26$  vs. their assumed  $\alpha = -1.6$  (Sawicki & Thompson 2006). Because of our Steidel-like sample selection combined with an unprecedented wide range of tests that we carried out on our sample, our LF measurements are uniquely robust against systematic effects. Details of the KDF observations and LF measurements are given in Sawicki & Thompson (2005) and Sawicki & Thompson (2006), respectively, and are briefly reviewed in § 2. The purpose of the present paper is to explore how these new, more accurate, shallower LFs impact our view of the cosmic UV luminosity density and star formation history of the Universe, by taking proper account of the evolving number density of faint, sub- $L^*$  galaxies.

As in all the papers in the KDF series, in the present paper we use the AB flux normalization (Oke, 1974) and adopt  $\Omega_M=0.3$ ,  $\Omega_\Lambda=0.7$ , and  $H_0=70$  km s $^{-1}$ Mpc $^{-1}$ . We also define the characteristic magnitude  $M_{LBG}^*\equiv -21.0$ , and a corresponding characteristic luminosity  $L_{LBG}^*$ . These parameters correspond very closely to the value of  $M^*$  at  $z\sim 3$  and  $z\sim 4$  as measured by us in the KDF (Sawicki & Thompson 2006) and at  $z\sim 3$  by Steidel et al. (1999).

## 2. THE KDF GALAXY SAMPLE AND LUMINOSITY FUNCTIONS

In this section we briefly summarize some of the most important features of the KDF data on which we base our analysis. A detailed description of the Keck Deep Field observations, data reductions, and high- $z$  galaxy selection can be found in Sawicki & Thompson (2005), while our  $z\sim 4$ , 3, and 2 luminosity function measurements are presented and discussed in detail in Sawicki & Thompson (2006).

### 2.1. The KDF survey

Our analysis is based on results from our very deep multicolor imaging survey carried out using a total of 71 hours of integration on the Keck I telescope. These Keck Deep Fields use the same  $U_nGRI$  filter set and color-color selection techniques as are used for brighter LBGs in the work of Steidel et al. (1999, 2003, 2004). In contrast to the Steidel et al. work, however, the KDFs reach  $\mathcal{R}_{lim}=27$ ; this is 1.5 magnitudes deeper than Steidel et al. surveys and significantly below  $L^*$  at  $z=2-4$ : even at  $z\sim 4$  we reach two magnitudes fainter than  $M^*$ . Furthermore, the KDFs have an area of 169 arcmin $^2$  divided into 3 spatially-independent patches on the sky — an arrangement that allows us to monitor the effects of cosmic variance on our results.

An important feature of the KDF is that our use of the  $U_nGRI$  filter set lets us select high- $z$  galaxies using the color-color selection criteria defined and spectroscopically tested by Steidel et al. (1999, 2003, 2004). We can thus confidently select sub- $L^*$  star-forming galaxies at high redshift without the need for spectroscopic charac-

terization of the sample — characterization that would be extremely expensive at the faint magnitudes that interest us. Moreover, this commonality with the Steidel et al. surveys has allowed us to reliably combine our data with theirs, thereby for the first time consistently spanning a large range in galaxy luminosity at high redshift.

To  $\mathcal{R}_{lim}=27$ , the KDF contain 427, 1481, 2417, and 2043  $U_nGRI$ -selected star-forming galaxies at  $z\sim 4$ ,  $z\sim 3$ ,  $z\sim 2.2$ , and  $z\sim 1.7$ , respectively, selected using the Steidel et al. (1999, 2003, 2004) color-color selection criteria. At our completeness limit, the KDF data probe galaxies with UV luminosities that correspond to star formation rates (uncorrected for dust obscuration) of only 1–2  $M_\odot/\text{yr}$ .

## 2.2. The $z\sim 2$ , 3, and 4 luminosity functions

Following Steidel et al. (1999), our LF calculation uses the effective volume technique, computing  $V_{eff}$  via recovery tests of artificial high- $z$  galaxies implanted into the images. To increase the luminosity range over which we can robustly study the high- $z$  LFs, at the bright end of the  $z\sim 3$  and  $z\sim 4$  samples we augmented our KDF data with the results of Steidel et al. (1999). Because of the identical filter set, object selection, and LF measurement technique, we can do this with little fear of introducing systematic offsets as can happen when other deep but relatively small-area surveys are augmented with shallower, wide-field data.

In Fig. 2 we reproduce the  $z\sim 4$ , 3, and 2.2 luminosity functions from Sawicki & Thompson (2006). In that paper we have examined a wide range of potential sources of systematic problems, including effects due to modeling of survey volume, differential sample selection, field-to-field variance, uncertainties in  $k$ -corrections, and so on. On the basis of these tests we have a very good understanding of the reliability of our LF results. In summary, we found that at  $z\sim 4$  and  $z\sim 3$ , our LF measurements are immune to a range of potential systematic effects, while our  $z\sim 2.2$  and  $z\sim 1.7$  LFs are more uncertain. The  $z\sim 1.7$  LF is likely quite strongly affected by systematics and so we do not include it in the analysis presented here. The  $z\sim 2.2$  LF measurement is *possibly* also affected by systematics but to a much smaller degree than the  $z\sim 1.7$  one: we can confidently state that the number density of  $z\sim 2.2$  galaxies is *not lower* than that shown in Fig. 2, and that if it is higher, it is higher by no more than a factor of  $\sim 2$ . The potential systematic error at  $z\sim 2.2$  is due to our uncertainty regarding the survey volume which itself stems from our uncertainty in the model colors of  $z\sim 2.2$  galaxies. The LF shown in Fig. 2 is based on our best and most realistic assumptions, namely that there is moderately strong dust obscuration of  $E(B - V)=0.15$ . The potentially twice-higher normalization would ensue in the extreme and rather unrealistic case of no dust (see Sawicki & Thompson 2006 for details) — a scenario that appears highly unlikely in view of recent spectral energy distribution studies (Shapley et al. 2005; Sawicki et al. 2006). It must be stressed again, however, that the  $z\sim 3$  and  $z\sim 4$  LFs, are *very* robust against such and other systematics.

The uncertainties in Fig. 2 include both  $\sqrt{N}$  statistical uncertainty in galaxy numbers and a measure of the effects of large scale structure (“cosmic variance”) obtained from a bootstrap resampling analysis of the mul-

tiples fields in the KDF. Both these sources of uncertainty are propagated into our error estimates for the luminosity density. We also note that at both  $z\sim 4$  and  $z\sim 3$ , we find  $M^*\approx -21.0$ , in good agreement with the  $z\sim 3$  Steidel et al. 1999 value converted into our cosmology. For convenience, we have thus defined a reference characteristic magnitude  $M_{LBG}^*\equiv -21.0$  and the equivalent characteristic luminosity  $L_{LBG}^*$ ; these values correspond to a galaxy with a (dust-free) star formation rate of 15  $M_\odot/\text{yr}$  (e.g., Kennicutt 1998).

In contrast to the Steidel et al. (1999) results, however, we find a somewhat shallower faint-end slope  $\alpha$ . At  $z\sim 3$  we find  $\alpha = -1.43$ , compared to their  $\alpha = -1.6$ , and at  $z\sim 4$  we find  $\alpha=-1.26$ . This evolving faint-end slope marks one of the most striking findings of the KDF to date: a differential, luminosity-dependent evolution of the Lyman Break Galaxy luminosity function. Simply put, while the number density of luminous galaxies ( $L>L^*$ ) remains fixed, the number density of sub- $L^*$  objects more than doubles from  $z\sim 4$  to  $z\sim 3$ . Our numerous tests show that this result is highly robust and insensitive to systematic biases (see Sawicki & Thompson 2006). In the present paper we turn to investigate how this differentially evolving galaxy population, reflected in an evolving luminosity function, impacts our view of the cosmic luminosity density and star formation rate density.

## 3. THE LUMINOSITY DENSITY

The luminosity density is the sum of all the light at a given wavelength, or range of wavelengths, from all galaxies in a unit volume. It can be computed as the luminosity-weighted integral of the galaxy luminosity function  $\phi(L)$ :

$$\rho_L = \int_0^\infty L\phi(L)dL, \quad (1)$$

which, for a luminosity function of the Schechter (1976) form,  $\phi(L)dL = \phi^*(L/L^*)^\alpha e^{-L/L^*} dL/L$ , can be expressed in terms of the gamma function,  $\Gamma(x) = \int_0^\infty e^{-t} t^{x-1} dt$ , as

$$\rho_L = \phi^* L^* \Gamma(\alpha + 2). \quad (2)$$

Because of the difficulty of constraining the number density of faint galaxies at high redshift, most studies focus on the partial, or incomplete, luminosity density — i.e., the luminosity density due to objects brighter than some limiting luminosity  $L_{lim}$ . We, too, will do so here at first by focusing on galaxies brighter than  $0.1L_{LBG}^*$  (§ 3.1) before presenting the *total* luminosity density (§ 3.2) and then examining the contributions to that total that are made by galaxies with luminosities in various luminosity bins (§ 3.3).

### 3.1. Luminosity in galaxies brighter than $0.1L_{LBG}^*$

Given a galaxy luminosity function  $\phi(L)$ , the luminosity density due to galaxies brighter than  $L_{lim}$  is

$$\rho_L(L > L_{min}) = \int_{L_{min}}^\infty L\phi(L)dL. \quad (3)$$

For the Schechter LF parametrization this can be expanded as

$$\rho_L(L > L_{min}) = \phi^* L^* [\Gamma(\alpha + 2) - \gamma(\alpha + 2, L_{min}/L^*)], \quad (4)$$

where  $\gamma(x, l) = \int_0^l e^{-t} t^{x-1} dt$  is the lower incomplete gamma function (e.g., Arfken 1985, Press et al. 1986).

We adopt  $L_{lim}=0.1L_{LBG}^*$ , which corresponds to  $M_{1700}=-18.5$  or, in the absence of dust, a galaxy with a star formation rate of  $\sim 1.5 M_{\odot}/\text{yr}$  (Kennicutt 1998). As Fig. 1 shows, this choice of  $L_{lim}$  captures approximately 75% of the UV light at  $z\sim 4$  and 3 for the luminosity functions we measure in the KDF.

We show the  $\rho_L(L>0.1L_{LBG}^*)$  KDF values with filled circles in Fig. 3, together with GALEX values at lower redshift (filled squares) and Iwata et al. (2006a, 2006b) values at  $z\sim 5$  (filled triangle). Tables 1 and 2 list the values of luminosity density for the KDF and for other surveys. The KDF values were computed by applying Eq. 3 to the Schechter function parameters of Sawicki & Thompson (2006). The uncertainties associated with our KDF points in Fig. 3 (and in all subsequent figures) include the contributions of both Poisson statistics and cosmic variance, the latter estimated through bootstrap resampling of the five KDF fields. Also shown in Fig. 3 are the  $z\leq 1$  GALEX UV luminosity density values of Schiminovich et al. (2005) which we have translated from their 1500Å to 1700Å and adjusted to represent only galaxies brighter than  $0.1L_{LBG}^*$  by scaling their total luminosity densities using our Equations 3 and 1 together with the GALEX LF Schechter parameters given by Arnouts et al. (2005) and Wyder et al. (2005). The  $z\sim 5$  point is based on new work by Iwata et al. (2006a, 2006b), who select  $z\sim 5$  LBGs from Subaru Suprimecam data (the median redshift of their sample is  $z=4.8$ , but for simplicity we refer to it here as  $z\sim 5$ ). These new  $z\sim 5$  results build on earlier work by these authors (Iwata et al. 2003) and are the deepest and widest-area LF results presently available at  $z\sim 5$ , as they are drawn from a total of 1290 arcmin<sup>2</sup> and reach  $M_{LBG}^*+0.95$ , or 0.7 mag deeper than the  $z\sim 5$  LFs of Ouchi et al. (2004). I. Iwata and his collaborators have kindly provided us with their new, deep estimates of  $z\sim 5$  incompleteness-corrected LBG number densities which they have computed using the  $V_{eff}$  approach similar to the one we used in the KDF (see Iwata et al. 2003 and I. Iwata in preparation for details). We then used these number densities to calculate the Schechter function parameters and their uncertainties following the same procedure as we used for our lower- $z$  KDF samples (see KDF II). We find  $M_{1700}^* = -20.80_{-0.40}^{+0.40}$ ,  $\log \phi^* = -3.10_{-0.30}^{+0.19}$ , and  $\alpha = -1.01_{-0.49}^{+0.50}$  at  $z\sim 5$  from the Iwata et al. data while the corresponding  $z\sim 5$  UV luminosity densities are given in Tables 1 and 2.

Several interesting trends are apparent in Fig. 3. First, it is clear that the luminosity density at  $z\sim 4$  is substantially lower than that at  $z\sim 3$ . This is a direct consequence of the shallower faint-end of the luminosity function that we find at  $z\sim 4$ . This drop in luminosity density at  $z\sim 4$  is in contrast to the  $z\sim 4$  result of Steidel et al. (1999; small star symbols), but this is because these authors *assumed* a steeper, non-evolving  $\alpha = -1.6$  faint-end slope at this redshift. Our KDF results, instead, show an evolutionary trend whereby the luminosity density increases with time from  $z\sim 4$  to  $z\sim 3$ . As we show in more detail in § 3.3, this trend is due to the evolution of the population of sub- $L_{LBG}^*$  galaxies. It is not clear whether this evolutionary trend continues to  $z\sim 2$ ,

or whether there is a plateau in the luminosity density at  $z\sim 3-1$ . Our data favor a plateau, but a peak at  $z\sim 2$  cannot be fully ruled out due to potential systematic problems at that redshift (see § 2.2 and Sawicki & Thompson 2006 for details).

It also appears plausible that the evolution we see at  $z\sim 4\rightarrow 3$  in the KDF data may have started at earlier times: if we consider the Iwata et al. (2006)  $z\sim 5$  result then there appears to be a monotonic increase in the luminosity density produced by galaxies brighter than  $0.1L_{LBG}^*$  that extends from very early times, at least  $z\sim 5$ , until at least  $z\sim 3$ .

The GALEX points illustrate the now well-known drop in luminosity density from  $z\sim 1$  to  $z\sim 0$ . Together with our KDF results at  $z\sim 4, 3$ , and 2, and the Iwata et al. results at  $z\sim 5$ , the following trend is clear: the luminosity density, at least in galaxies brighter than  $0.1L_{LBG}^*$ , increases steadily from the earliest redshifts until at least  $z\sim 3$ ; it then culminates somewhere between  $z\sim 3$  and  $z\sim 1$  as either a peak or a broad plateau; and it then drops precipitously from  $z\sim 1$  to  $z\sim 0$ . This picture is consistent with that first presented by Sawicki et al. (1997), who found a broad peak in the luminosity density at  $z\sim 2.5$  and an onset of cosmic star formation at  $z>3.5^3$ .

### 3.2. The total luminosity density

Our analysis thus far (summarized in Fig. 3), has concerned itself with luminosity density due to galaxies brighter than  $0.1L_{LBG}^*$  only. This is an approach common in the literature, but one that does not present a complete census of the cosmic luminosity density. We thus now turn to the question of how our results change if we incorporate the contribution of extremely faint galaxies,  $L<L_{LBG}^*$  — galaxies that are too faint to be seen in *any* of the surveys to date at high redshift, including ours.

The *total* luminosity density is obtained by integrating the luminosity function over *all* luminosities from 0 to  $\infty$  (Eq. 1). This calculation involves an extrapolation to magnitudes fainter than our limiting magnitudes, but the depth of our KDF data allows this to be a robust extrapolation: (1) because of their large area and depth the KDFs have constrained the LFs' faint-end slopes sufficiently well, and, (2) the depth of our data is such that the extrapolation involves only  $\sim 25\%$  of the total light (Fig. 1). Similar remarks apply to the surveys of Iwata et al. (2006) at  $z\sim 5$  and GALEX at  $z\lesssim 1$ . Surveys with smaller areas and/or shallower limiting magnitudes must make much bigger and more uncertain corrections, but this is not the case for the KDF.

The *total* luminosity densities are shown in Fig. 4 with open symbols and are compared with  $L>0.1L_{LBG}^*$  results of § 3.1 that are represented by filled points. The difference between the  $L>0.1L_{LBG}^*$  and the total results is very small at high redshift,  $z\geq 2$ . This is so because the faint-end slopes measured by us in the KDF (and by Iwata et al. 2006 at  $z\sim 5$ ) are relatively shallow, resulting in relatively little additional light in galaxies fainter than  $0.1L_{LBG}^*$ . However, although the effect is small here, the importance of reliably measuring the faint end slope of

<sup>3</sup> We note that Madau et al. 1996 presented only lower limits on the high-redshift luminosity densities and that these values were corrected for incompleteness only later in Madau et al. 1998.

the LF cannot be understated: had the faint-end slopes turned out to be significantly steeper, much stronger differences would have ensued. As it is, most of the light at high redshift resides in galaxies with  $L=0.1-1L_{LBG}^*$  (as we show in § 3.3), underscoring the importance of accurately measuring the LF's faint end slope at luminosities fainter than  $L_{LBG}^*$ . At lower redshifts,  $z \leq 1$ , there is a fairly significant difference between the total and the  $L > 0.1L_{LBG}^*$  values. However, this is not because the low- $z$  faint-end slope is very steep (it isn't), but primarily because at  $z \leq 1$   $L^*$  is a magnitude or more fainter than our fixed high- $z$   $L_{LBG}^*$ . This difference ensures that the  $0.1L_{LBG}^*$  limit of § 3.1 does not encompass most of the low- $z$  light.

At  $z \leq 1$  the total UV luminosity becomes dominated by very faint galaxies, galaxies with luminosities below  $0.1L_{LBG}^*$  (see Fig. 5). It is curious to note that the total luminosity density at  $z \sim 0.5$  is similar to that at  $z \sim 4$ , which is not the case when the comparison is restricted to galaxies brighter than  $0.1L_{LBG}^*$  only. Nevertheless, while the decline from  $z \sim 1$  to  $z \sim 0$  is less precipitous when one considers the *total* luminosity density rather than just that due to galaxies brighter than  $0.1L_{LBG}^*$ , the broad qualitative picture is the same in both cases: a gradual build-up in the luminosity density from very high redshift which is followed by a peak or a plateau between  $z \sim 3$  and  $z \sim 1$  which in turn is followed by a decline to  $z \sim 0$ .

This broad qualitative picture is also only mildly affected when one corrects for the effects of interstellar dust. Here, at each redshift we have applied a *range* of plausible dust corrections and the resulting dust-corrected star formation rate densities are shown as a gray band in Fig. 4. We corrected the  $z \geq 2$  values by factors of 5–15 as suggested by various studies of extinction in Lyman Break Galaxies (e.g., Sawicki et al. 1998; Papovich et al. 2001; Shapley et al. 2001, 2005; Vijh, Witt, & Gordon 2003; Reddy & Steidel 2004; Iwata et al. 2005) and the  $z < 2$  GALEX values by 2–5 (Schiminovich et al. 2005; see also, e.g., Tresse et al. 2002; Pérez-González et al. 2003). After applying dust corrections we can now properly regard Fig. 4 as showing us the cosmic star formation rate history of UV-bright galaxies.

Extremely dust-obscured galaxies such as high- $z$  SCUBA sources (e.g., Smail et al. 1997; Barger et al. 1998; Eales et al. 1999; Chapman et al. 2005) are not included in the dust-corrected star formation rate densities shown in Fig. 4. Most such galaxies have UV luminosities that heavily underrepresent their star formation rates and thus such galaxies are not properly included if our census is to be regarded as a measurement of star formation activity in the Universe. The number density of such heavily obscured sources at *low redshift* is too low to make a large contribution to the star formation rate density. However, at high redshift,  $z \sim 2$ , their numbers are sufficiently large that their contribution is significant and including them in our census would raise the star formation rate density shown in Fig. 4. The increase would be highest at  $z \sim 2$  where the redshift distribution of SCUBA sources appears to peak (Chapman et al. 2005). The correction to the star formation rate density at that epoch may be up to a factor of two, i.e., 0.3 in dex (Chapman et al. 2005; Reddy et al. 2005).

Taken together, however, the incorporation of dust cor-

rections — be they only dust corrections to the UV-selected galaxies or also the inclusion of the contribution of heavily-obscured sources — does not qualitatively affect the picture shown in Figs. 3 and 4. Dust or no dust, the star formation rate density of the universe apparently began rising at some high redshift  $z \gtrsim 4$ , continued to rise until at least  $z \sim 3$ , climaxed in a peak or a plateau between  $z \sim 3$  and  $z \sim 1$ , and then dropped to  $z \sim 0$ .

While the decline from  $z \sim 1$  to the present epoch has been well established for a long time (e.g., Lilly et al. 1996; Schiminovich et al. 2005), the behavior of the cosmic star formation rate density at  $z \gtrsim 3$  was less clear: the Steidel et al. (1999) picture of a plateau extending from  $z \sim 3$  to  $z \sim 4$  and possibly beyond (e.g., Giavalisco et al. 2004b; Ouchi et al. 2004) was for a long time the gold standard in the field. However, the Steidel et al. (1999) no-evolution result was based on the measurement of a non-evolving LF's bright end and the *assumption* of a non-evolving faint-end. Our KDF results clearly show that, in contrast to these assumptions, the luminosity function evolves and this evolution is reflected in the luminosity density which evolves with time at high redshift.

### 3.3. Dependence on galaxy luminosity

In the previous Section we have shown that the UV luminosity density exhibits a rise from early epochs to  $z \sim 3$ , a peak or plateau between  $z \sim 3$  and  $z \sim 1$ , and then a decline to  $z \sim 0$ . We now ask the question: which galaxies are responsible for this picture? To address this question we split our analysis into three luminosity intervals, computing the luminosity density in galaxies brighter than  $L_{LBG}^*$ , galaxies between  $L_{LBG}^*$  and  $0.1L_{LBG}^*$ , and those fainter than  $0.1L_{LBG}^*$ .

The luminosity density due to just those objects with luminosities in the range  $L_{max} > L > L_{min}$  is given by

$$\begin{aligned} \rho_L(L_{max} > L > L_{min}) &= \int_{L_{min}}^{L_{max}} L \phi(L) dL \quad (5) \\ &= \phi^* L^* [\gamma(\alpha + 2, L_{min}/L^*) \\ &\quad - \gamma(\alpha + 2, L_{max}/L^*)]. \end{aligned}$$

We make the boundaries of our luminosity intervals at  $L_{LBG}^*$  and at  $0.1L_{LBG}^*$ . Note that to compute the last (faintest) of those three intervals we must extrapolate the faint-end slope of the LF at all redshifts, but the data we consider here (the KDF, GALEX, and the  $z \sim 5$  Subaru data of Iwata et al. 2006) all go sufficiently deep to measure the faint-end slopes well, thus making these extrapolations acceptable.

In Fig. 5 we plot the redshift evolution of the luminosity-dependent luminosity densities (colored symbols and lines) compared with the *total* luminosity density from Fig. 4 in § 3.2 (open circles and black line). At high redshift,  $z > 2$ , the luminosity density is dominated by galaxies in the narrow luminosity range  $(0.1-1)L_{LBG}^*$ : galaxies that are brighter than  $L_{LBG}^*$  or those that are fainter than  $0.1L_{LBG}^*$  contribute relatively little light to the total at these redshifts! In contrast there is little evolution in the bright end of the galaxy population between  $z \sim 2, 3, \text{ and } 4$  (and 5) and this results in a nearly constant luminosity density of bright, super- $L_{LBG}^*$  galaxies over  $z \sim 2-5$ . To date, most of the focus at high redshift has been on galaxies around  $L_{LBG}^*$ . But it is the sub- $L^*$  galaxies that, as we have illustrated here, dominate

the total luminosity density at  $z \gtrsim 2$ . This dominant sub-population is only now for the first time starting to be robustly probed by our KDF survey and by follow-up studies that are now either underway or being planned.

We conclude this section by summarizing our main points. At high redshift,  $z > 2$ , there is a rise in the total luminosity density with time. This rise is not due to changes in the population of bright galaxies,  $L \gtrsim L_{LBG}^*$ , but is instead directly related to the rise in the number density of faint, sub- $L_{LBG}^*$  galaxies and the steepening of the faint end slope of the luminosity function that reflects it.

#### 4. DISCUSSION

##### 4.1. Comparison with other work

In this section we compare our results with those of other surveys. Figure 3 shows results from several other programs that recently studied the cosmic UV luminosity density at high redshift. We consider here a number of recent surveys, but — with the exception of the work of Steidel et al. (1999) — we avoid results that are based on the very small area HDFs (e.g., Madau et al. 1996; 1998; Sawicki et al. 1997; Connolly et al. 1997; Arnouts et al. 2005) because such results have to be held suspect given the small field of view of the HDFs and the resulting susceptibility to cosmic variance. We have, however, included some  $z \sim 6$  results based on the small Hubble Ultra Deep Field since there are at present no other data that probe significantly below  $L_{LBG}^*$  at that redshift. In all the surveys that we do consider we have converted the published results to a consistent limiting depth of  $L = 0.1 L_{LBG}^*$  and have adjusted them to rest-frame 1700Å values as necessary. The superiority of the KDF results vis-a-vis these other surveys lies in the combination of the KDF's superb depth, large field of view, multiple sightlines, well-understood sample selection, and an extensive range of robustness-gauging tests that we carried out as part of our LF measurement (Sawicki & Thompson 2006).

##### $z \sim 2$ and $z \sim 3$

At  $z \sim 2$  and  $z \sim 3$  our KDF results are in very good agreement with other available measurements, namely the photometric redshift results of Gabasch et al. (2004b) and the LBG work of Steidel et al. (1999).

The agreement with Steidel et al. (1999)  $z \sim 3$  results is — at one level — not surprising because the KDF uses the very same filter set and sample selection as the ground-based Steidel et al. surveys. Indeed — our  $z \sim 3$  and  $z \sim 4$  luminosity functions incorporate Steidel et al. (1999) data at the bright end (see Sawicki & Thompson 2006). On the other hand, however, Steidel et al. (1999) used the Hubble Deep Field to constrain the shape of their luminosity function below  $M_{LBG}^* + 1$ , thereby incurring the uncertainty of differential selection between their bright and faint galaxies, in addition to potential cosmic variance issues due to the HDF's small area. Although there is a small difference between our and their faint-end LF slopes at  $z \sim 3$  (our  $\alpha = -1.43$  vs. their  $\alpha = -1.6$ ), there is quite good agreement between the luminosity densities at  $L < 0.1 L_{LBG}^*$ .

Our KDF results are also in excellent agreement with the  $z \sim 2$  and  $z \sim 3$  FORS Deep Field (FDF) and Great

Observatories Origins Deep Survey South (GOODS-S) results of Gabasch et al. (2004b). The FDF is a single relatively small ( $\sim 40$  arcmin<sup>2</sup>) deep field with sample selection (full-blown photometric redshifts) that is rather different than ours. Their GOODS-S data uses similar sample selection and area ( $\sim 50$  arcmin<sup>2</sup>) as the FDF but is a magnitude shallower than their FDF data, reaching only  $\sim M_{LBG}^* + 1$  at  $z \sim 3$  — depths comparable to those reached from the ground by Steidel et al. (1999). Despite the differences in sample selection and the relatively small area of their significantly deep data (the FDF), there is very good agreement between the luminosity densities they find and those that we find in the KDF.

Overall, all three results (KDF, Gabasch et al. 2004b, and Steidel et al. 1999) are highly consistent with each other, albeit ours is the most robust of the three given the KDF's large area and multiple sightlines (important for mitigating the effects of cosmic variance) combined with faint limiting magnitude (vital for constraining the faint end of the galaxy population), and extensive LF robustness tests.

##### $z \sim 4$

At  $z \sim 4$  we compare our results with Subaru Deep Survey (SDS) work of Ouchi et al. (2004), Giavalisco et al. (2004b) results based on the Great Observatories Origins Deep Survey (GOODS; Giavalisco et al. 2004a) HST data, as well as the aforementioned work of Gabasch et al. 2004b and that of Steidel et al. (1999). At  $z \sim 4$ , the GOODS-S component of the Gabasch et al. (2004b) analysis reaches only  $\sim M_{LBG}^* + 0.5$ , so here we consider their work to be based primarily on the single-pointing FORS Deep Field. All the surveys considered use variants of the Lyman Break color-color selection technique, with the exception of the FDF, which uses full photometric redshifts.

These four surveys (Ouchi et al. 2004; Gabasch et al. 2004b; Giavalisco et al. 2004; and Steidel et al. 1999) do not present a consistent picture, giving a range of luminosity densities that span a factor of  $\sim 2.5$ . Let us examine the differences in more detail.

Gabasch et al. (2004b) do not give FDF luminosity density measurements at  $z \sim 4$  but present values at  $z = 3.5$  and 4.5 (see Fig. 3). However, these values bracket our  $z \sim 4$  KDF result and a straightforward interpolation between their FDF  $z = 3.5$  and  $z = 4.5$  points is in very good agreement with our data. This agreement is to be expected given the good agreement between our LFs and theirs (see Sawicki & Thompson 2006), but note that our KDF result is much more robust for reasons outlined in § 4.1.0.

The results of Steidel et al. (1999) at first appear to be somewhat higher than ours, but this is because of their *assumption* that the faint end of the LF does not evolve from  $z \sim 3$ . With a shallower faint-end  $\alpha$  at  $z \sim 4$ , as found in the KDF, their results would be in agreement with ours.

Giavalisco et al. (2004b) give two measurements from the GOODS data, obtained using two different techniques. One measurement (from their  $\chi^2$  technique) paints a picture of a luminosity density that does not differ from that at  $z \sim 3$ , while the other (from their  $V_{eff}$  approach) yields an evolving luminosity density, in agree-

ment with our results. Giavalisco et al. prefer their  $\chi^2$  method and results, but our KDF data are in much better agreement with their lower,  $V_{eff}$  point.

The SDS work of Ouchi et al. (2004) gives the highest luminosity density value but this value may well be prejudiced by potential problems with their measurement of the LF's faint end: at  $z\sim 4$  their data probes one magnitude fainter than  $M_{L_{BG}}^*$  and they find an extremely steep faint-end slope of  $\alpha=-2.2$  that gives an infinite total luminosity density (Eq. 1). A strong limitation of their work is that their color selection is not well calibrated spectroscopically except for a handful of redshifts and must instead rely heavily on models of galaxy colors. It is not clear how strong are the systematic effects inherent in this modeling.

Overall, our results are in very good agreement with those from the FDF and with the GOODS  $V_{eff}$  approach, while we find substantially less luminosity than does the SDS and the GOODS  $\chi^2$  approach. We feel that, given the robustness of our sample selection and LF measurement, our results are the most reliable of all those currently available at  $z\sim 4$ .

#### 4.2. Earlier epochs

$z\sim 5$

The literature now contains several measurements of the luminosity function and cosmic luminosity density at  $z\sim 5$ . Here we discuss those by Iwata et al (2006) as well as those based on GOODS (Giavalisco et al. 2004b), SDS (Ouchi et al. 2004), and FDF (Gabasch et al. 2004a, 2004b; note that the FDF results are at  $z\sim 4.5$ ). With the exception of the Giavalisco et al. GOODS results, all these surveys present both luminosity densities and luminosity functions; of these, the Iwata et al. (2006) Subaru work has the best combination of depth (0.7 mag deeper than the SDS) and area (an order of magnitude larger than the FDF).

The Iwata et al. (2006), FDF, and the GOODS  $V_{eff}$  results all indicate that the luminosity density at  $z\sim 5$  is lower than that at  $z\sim 4$  in the KDF. In both the Subaru work of Iwata et al. (2006) and in the FDF (Gabasch et al. 2004a) the faint-end slope of the LF is quite shallow at these redshifts, in apparent continuation of the LF evolutionary trend that we see in the KDF. It is this shallow faint-end slope that results in the low luminosity density that these surveys measure at  $z\sim 5$ . On the other hand, the GOODS  $\chi^2$  results as well as those from the SDS would suggest a higher luminosity density — one that is almost unchanged from  $z\sim 3$ . In the SDS work this is caused by a very steep faint-end slope that they assume from their lower- $z$  results (their observations at  $z\sim 5$  reach only to  $L_{L_{BG}}^*+0.25$ ). The  $z\sim 3\rightarrow 4$  trend seen in the KDF tends to favor a continuing drop in the luminosity density to higher redshifts, in line with the Iwata et al. (2006), FDF, and GOODS- $V_{eff}$  values.

$z\sim 6$

The situation at  $z\sim 6$  is tenuous despite much recent effort. Some recent results (Bouwens et al. 2006; the  $\chi^2$  GOODS results of Giavalisco et al. 2004b) suggest a  $z\sim 6$  luminosity density nearly as high as that at  $z\sim 3$ . Others, (Bunker et al. 2004;  $V_{eff}$  results of Giavalisco et al. 2004b) give values that are significantly lower (see

Fig. 3).

The situation is tenuous for several reasons. First, at  $z\sim 6$  sample selection is generally done using just one color,  $i-z$ , which makes it difficult to estimate redshift distributions, and hence survey volumes, and hence source number densities. The absence of a third, redder band also makes source luminosities *very* uncertain because at  $z\sim 6$  the  $z$ -band fluxes that are invariably the starting point for computing luminosities are attenuated by intergalactic hydrogen line blanketing. While corrections for this attenuation are usually applied, such corrections are necessarily statistical because they rely on an *average* rather than exact distribution of intervening gas, and so are subject to systematic biases that are difficult to quantify. Moreover, these corrections are typically based on the models of Madau (1995); these models are based on lower-redshift data, and it is unclear how well they work at  $z\sim 6$ . It is thus not clear how well the fluxes and hence luminosities of  $z\sim 6$  candidates are being estimated.

Another limitation is that the all-important shape of the faint end of the  $z\sim 6$  luminosity function is highly uncertain. Assuming the Steidel et al. (1999)  $z\sim 3$  faint-end slope of  $\alpha=-1.6$  is not a good approach in light of the fact that the true slope is shallower even at  $z\sim 3$  and that it becomes progressively shallower with increasing redshift (Sawicki & Thompson 2006; see also Gabasch et al. 2004a). On the other hand, empirically constraining the number density of sub- $L_{L_{BG}}^*$  galaxies from the data is highly problematic since the only field sufficiently deep for this task is the Hubble Ultra Deep Field (UDF). The UDF's small area (12 arcmin<sup>2</sup>) makes it subject to potential cosmic variance effects only slightly less severe than those affecting the HDFs. Bouwens et al. (2006) argue that cosmic variance effects on UDF scales are not large at  $z\sim 6$  (they suggest a 35% RMS effect), but this seems questionable: e.g., the difference in comoving luminosity density at redshifts  $z\sim 3$  and  $z\sim 4$  between the two  $\sim 5$  arcmin<sup>2</sup> Hubble Deep Fields is a factor of two (e.g., Ferguson, Dickinson, & Williams 2000) and it is reasonable to suppose that similarly large fluctuations can be present on the just slightly larger scale of the UDF.

In summary, present measurements of the  $z\sim 6$  UV luminosity density are highly uncertain. Given that our KDF data show that luminosity density is dropping already from  $z\sim 3$  to  $z\sim 4$ , it seems unlikely that it would be as high at  $z\sim 6$  as it is at  $z\sim 3$ . A simple extrapolation of the trend we see between  $z\sim 3$  and  $z\sim 4$  in the KDF — a trend that seems to continue to  $z\sim 5$  in the work of Iwata et al. 2006 — suggests the cosmic UV luminosity density at  $z\sim 6$  is similar to that reported by Bunker et al. (2004). To make further progress on this issue will require large, multi-field  $z\sim 6$  galaxy samples with  $J$ -band photometry that reaches significantly below  $L_{L_{BG}}^*$ .

#### 4.3. Keeping the Universe ionized

Recently there has been much interest in the question of the objects that are responsible for reionizing the Universe at high redshift (e.g., Lehnert & Bremer 2003; Bunker et al. 2004; Martin & Sawicki 2004; Stivelli, Fall, & Panagia, 2004; Yan & Windhorst 2004). Several of these authors have concluded that the number of luminous galaxies at  $z\sim 6$  is insufficient to provide enough photons to keep the Universe ionized and have

postulated that sub- $L^*$  galaxies that are largely too faint to be observed directly at these redshifts may make up the deficit. The KDF’s highest redshift bin is at  $z\sim 4$ , only 0.7 Gyr after the putative redshift of reionization at  $z=6.5$ , and since our survey probes significantly below  $L_{LBG}^*$ , we are in a good position to comment on the issue. We will study here whether faint galaxies produce enough ionizing photons to maintain ionization at  $z\sim 4$  and later, and ask what that tells us about keeping the Universe ionized at earlier epochs.

Following much of the  $z\sim 6$  work (e.g., Ferguson, Dickinson, & Papovich 2002; Bunker et al. 2004; Yan & Windhorst 2004; Bouwens et al. 2006), our estimate will be based on the Madau, Haardt, & Rees (1999) radiative transfer calculation. As we mention later, this is not necessarily the best approach to adopt, but it is the approach taken by most observers so for consistency we, too, will use it here.

According to Madau, Haardt, & Rees (1999), the rate of production of ionizing photons needed to maintain ionization at a given redshift can be expressed as

$$\begin{aligned} \dot{N}_{ion}(z) &= \frac{\bar{n}_H(0)}{\bar{t}_{rec}(z)} \\ &= \left( \frac{1.58 \cdot 10^{51}}{\text{s} \cdot \text{Mpc}^3} \right) C_{30} \left( \frac{1+z}{6} \right)^3 \left( \frac{\Omega_b h_{70}^2}{0.041} \right)^2 \end{aligned} \quad (6)$$

where  $\bar{n}_H(0)$  is the average density of hydrogen,  $\bar{t}_{rec}(z)$  is the average recombination time,  $C_{30}$  is the clumping factor of ionized hydrogen,  $\Omega_b$  is the baryon density, and  $h_{70}$  is Hubble’s constant in units of  $70 \text{ km s}^{-1} \text{ Mpc}^{-1}$ . It should be noted that Madau et al.’s  $C_{30}=1$ , motivated by simulations by Gnedin & Ostriker (1997), is likely too high and more recent studies suggest reionization is somewhat easier to achieve (see, e.g., Miralda-Escudé 2003; Furlanetto & Oh 2005; Meiksin 2005). At rest-frame  $1700\text{\AA}$ , we are measuring photon energies that are too low to ionize hydrogen and so we need to relate our  $1700\text{\AA}$  luminosity densities to number densities of  $\lambda=0\text{--}912\text{\AA}$  photons. Using the Starburst99 evolutionary spectral synthesis models (Leitherer et al. 1999) we find that the rate of production of ionizing photons,  $\dot{N}_{ion}$ , is related to the  $1700\text{\AA}$  luminosity  $L_{1700}$  by

$$\dot{N}_{ion} = 1.64 \cdot 10^{25} \frac{L_{1700}}{\text{erg} \cdot \text{Hz}^{-1}}. \quad (7)$$

Equation 7 is valid for starbursts with age  $>10^7 \text{ yr}$ , Salpeter (1955) stellar initial mass function (IMF) with  $100 > M/M_\odot > 0.1$ , and is insensitive to metallicity. Then, combining Equations 6 and 7 we find that if the Universe is to be kept ionized by ongoing star formation, we need to have a  $1700\text{\AA}$  luminosity density of no less than

$$\frac{L_{1700}^{crit}(z)}{\text{erg} \cdot \text{s}^{-1} \text{Hz}^{-1} \text{Mpc}^{-3}} = 9.63 \cdot 10^{25} \frac{C_{30}}{f_{esc}^{rel}} \left( \frac{1+z}{6} \right)^3 \left( \frac{\Omega_b h_{70}^2}{0.041} \right)^2. \quad (8)$$

We have included in Eq. 8 a relative escape fraction term  $f_{esc}^{rel}$ , which accounts for the fact that in practice, due to various radiative transfer effects, fewer ionizing photons escape a galaxy than would be straightforwardly predicted by the number of escaping *non*-ionizing photons. There is currently much uncertainty about the escape fraction of ionizing radiation, but it seems reasonable that  $f_{esc}^{rel} \lesssim 0.5$  (Heckman et al. 2001; Steidel, Pettini,

& Adelberger 2001; Fernández-Soto, Lanzetta, & Chen 2003; Inoue et al. 2005), and certainly  $f_{esc}^{rel} \leq 1$  since the relative escape fraction cannot exceed unity.

The amount of UV starlight needed to keep the Universe ionized (as predicted by Equation 8) is shown as a solid gray curve in Figs. 3 and 4 for hydrogen clumping factor value of  $C_{30}=1$  and a conservative escape fraction  $f_{esc}^{rel}=0.5$ . Lower escape fractions would push the curve upwards while lower clumping factors,  $C_{30}<1$ , would lower it. As has been pointed out by a number of authors,  $z\sim 6$  galaxies brighter than  $0.1L_{LBG}^*$  do not produce enough UV light to ionize the Universe (Fig. 3). However, it would seem that there isn’t enough starlight to keep the Universe ionized even at  $z\sim 4$ , and this is so not only if we restrict ourselves to galaxies brighter than  $0.1L_{LBG}^*$ , but even if we integrate down the luminosity function all the way to  $L=0!$

In the calculation presented here, an unevolving  $z\sim 4$  galaxy population would clearly not be sufficient to maintain ionization at  $z\sim 6$ , and yet our observations indicate that the galaxy population is evolving, with the UV luminosity density dropping with increasing redshift. While at  $z\sim 4$  additional radiation from active galactic nuclei (AGN) might be enough to make up the deficit (but see Steidel et al. 2001), this is unlikely to be the case at higher redshifts as the number density of even low-luminosity AGN is decreasing with increasing lookback time (e.g., Willott et al. 2005). It would thus seem that the Universe cannot produce enough ionizing radiation either from stars or black holes to reionize its gaseous content at  $z\sim 6$ .

There are several ways out of this apparent paradox but ionizing radiation from very faint but otherwise “normal” star-forming galaxies does not appear to be one of them. Some possibilities include a radically non-standard IMF or stars with very low, nearly primordial metallicities (e.g., Bunker et al. 2004; Stiavelli, Fall, & Panagia 2004). A less radical alternative, however, is that the Madau et al. (1999) requirement for reionization that is assumed by most observers is overly strict. There is an ongoing debate about the number of photons needed for reionization, a debate that is related to the uncertainty in the clumpiness of the intergalactic medium that controls the importance of recombinations (e.g., Madau et al. 1999; Miralda-Escudé 2003; Furlanetto & Oh, 2005; Meiksin 2005). It now seems highly plausible that the  $C_{30}=1$  assumed by Madau et al. (1999) and subsequently by many observers is significantly too high. If, for example, we follow the results of Meiksin (2005) instead of those of Madau et al. (1999) then the required  $L_{1700}^{crit}$  is a factor of  $\sim 5$  lower than that shown in Figs. 3 and 4. Under these less restrictive clumping assumptions massive stars in faint galaxies that follow the even relatively shallow faint-end LF slope we find in the KDF can produce more than enough ionizing photons at  $z\sim 4$  and plausibly also at higher redshifts. In this case, there is no need to invoke a very numerous faint population and steep LF faint-end slope at  $z\sim 6$ .

#### 4.4. The galaxies that dominate the UV luminosity density at high redshift

The steep increase in the total luminosity density with time at high redshift is caused by the increase in the number density of sub- $L_{LBG}^*$  galaxies and the associ-

ated steepening of the LF's faint-end slope. However, while the faint end of the luminosity function evolves, the bright end stays nearly constant — a fact that is reflected in the relative flatness of the luminosity density due to  $L > L_{LBG}^*$  galaxies. This differential evolution suggests that individual galaxies themselves are evolving and that they are doing so differentially with luminosity.

The evolutionary behavior of the differential luminosity density that we see over  $z \sim 5 \rightarrow 0$  (Fig. 5) is reminiscent of the galaxy downsizing picture (e.g., Cowie et al. 1996, Iwata et al. 2006a). Here, the epoch of vigorous star formation in the most luminous galaxies — those with  $L > L_{LBG}^*$  — ends first with a rapid decline in their activity starting at  $z \sim 2$ . This is followed at later epochs by a drop in the activity due to intermediate-luminosity galaxies ( $L = 0.1 - 1 L_{LBG}^*$ ). This in turn is followed by the dominance of those galaxies in our faintest luminosity bin —  $L < 0.1 L_{LBG}^*$ . However, unlike in the lower-redshift work of Cowie et al. (1996), here, at higher redshifts, the downsizing picture is so far only seen in luminosity and it remains to be seen if it is also tied to galaxy masses.

The differential evolution we observe in the luminosity density and the luminosity function must reflect evolution of individual galaxies. However, at present the mechanism for this evolution remains unknown. In Sawicki & Thompson (2006) we have suggested several possible mechanisms related to changes in timescales of star-forming episodes, or evolution in the amount or distribution of their interstellar dust. It is also possible that we are witnessing two different evolutionary mechanisms that dominate the different ends of the luminosity function and are competing around the characteristic LF luminosity  $L^*$ . It is possible, for example, that on the two different sides of  $L^*$  we are seeing galaxies that are governed by two different regimes of feedback — e.g., AGN feedback in more massive (and plausibly more luminous) galaxies, and star-formation-driven feedback in lower-mass (and lower luminosity) systems.

We are now working to understand the nature of the evolution we see by studying differences in the properties of *individual* galaxies as a function of epoch and luminosity. Clustering and spectral energy distribution studies will let us constrain the dark halo and stellar masses of galaxies as a function of luminosity, and thus will tell us whether the downsizing we see is related to galaxy masses as it seems to be at lower redshifts (Cowie et al. 1996). SED studies will also let us test whether other galaxy properties, such as their dust properties or timescales of their starbursting episodes vary with luminosity and epoch and thus whether they are responsible for the evolution we see. While observationally expensive, such differential comparisons of faint members of a population with their brighter brethren can lead to important insights (see, e.g., Sawicki et al. 2005) and will be key to understanding what drives the evolution of galaxies at high redshift.

## 5. SUMMARY AND CONCLUSIONS

Our KDF survey has allowed us to make the best measurement thus far of the UV luminosity density at  $z \sim 4, 3,$  and  $2$ . This is the case because our work builds directly on the well-tested photometric selection techniques of Steidel et al. (1999, 2003, 2004), because it probes very deep into the galaxy luminosity function, and because it

does so using several spatially independent fields to control for the effects of cosmic variance. The main results of our analysis of the UV luminosity density are:

1. The picture of *total* UV luminosity density, i.e., luminosity density due to galaxies of all luminosities, is that of a rise from early epochs,  $z \geq 4$ , followed by either a plateau or a broad peak at  $z \sim 3-1$ , and then followed by a decline to  $z=0$ . This picture is consistent with that presented by Sawicki et al. (1997), although is at odds with some recent work that posits a constant luminosity density over  $z \sim 6-1$ .
2. The luminosity density at high redshift,  $z \sim 2-4$ , is dominated not by luminous galaxies, but by sub- $L_{LBG}^*$  galaxies, where  $L_{LBG}^*$  is the characteristic 1700Å luminosity that corresponds to  $M_{LBG}^* = -21.0$ . Indeed, it is galaxies within a rather narrow luminosity range  $L = 0.1 - 1 L_{LBG}^*$  that dominate at these redshifts and it is the rapid evolution of these galaxies that drives the evolution in the *total* UV luminosity density.
3. In contrast to  $z \gtrsim 2$ , at lower redshifts,  $z \lesssim 1$  the total UV luminosity density, as shown most recently by GALEX, is dominated by *very* faint galaxies with  $L < 0.1 L_{LBG}^*$ . The  $L = 0.1 - 1 L_{LBG}^*$  galaxies that dominated at  $z \gtrsim 2$  are still important but no longer dominant. This reversal in the luminosity of the galaxies that dominate the total luminosity density is reminiscent of galaxy downsizing, although the effect we see so far is a downsizing in UV luminosity rather than galaxy mass.
4. Several recent studies have suggested that at  $z \sim 6$  there are not enough luminous galaxies to maintain ionization of intergalactic gas and proposed that a large population of faint galaxies is needed for that task. Within the context of the most widely-used models, we find that there seemingly aren't enough bright *and* faint star-forming galaxies even as late as  $z \sim 4$  to maintain ionization, questioning the assumptions of these most widely-used models. Apparently the Universe must be easier to reionize than some recent studies have assumed.

In this paper we have shown that the total UV luminosity density of the Universe at high redshift is dominated by galaxies fainter than the  $L_{LBG}^*$  galaxies that have thus far drawn most of the community's attention. These sub- $L_{LBG}^*$  galaxies are, as we have also found in Sawicki & Thompson (2006), evolving rapidly as a population, while the population of their far better studied, more luminous cousins appears to remain unchanged with time. The question then becomes, what makes the high- $z$  galaxies brighter than  $L_{LBG}^*$  and those fainter than  $L_{LBG}^*$  so different. We will address this issue in the future by studying the clustering properties and stellar populations of these important systems.

We thank the time allocation committee for a generous time allocation that made this project possible and the staff of the W.M. Keck Observatory for their help

in obtaining these data. We are also grateful to Chuck Steidel for his encouragement and support of the KDF project, Jerzy Sawicki for many useful comments, Ikuru Iwata, Kouji Ohta, and their collaborators for sharing their new  $z\sim 5$  Subaru results in advance of publication and Crystal Martin and Peng Oh for useful discussions.

Finally, we wish to recognize and acknowledge the very significant cultural role and reverence that the summit of Mauna Kea has always had within the indigenous Hawaiian community; we are most fortunate to have the opportunity to conduct observations from this mountain.

## REFERENCES

- Arfken, G. 1985, *Mathematical Methods for Physicists* (San Diego: Academic Press, Inc.)
- Arnouts, S. et al. 2005, *ApJ*, 619, L43
- Baker, A. J., Lutz, D., Genzel, R., Tacconi, L. J., Lehnert, M. D. 2001, *A&A*, 372, 37
- Barger, A.J., et al. 1998, *Nature*, 394, 248
- Bouwens, R.J., et al. 2003, *ApJ*, 595, 589
- Bouwens, R.J., et al. 2004, *ApJ*, 606, L25
- Bouwens, R.J., Illingworth, G.D., Blakeslee, J.P., & Franx, M. 2006, *ApJ*, submitted, astro-ph/0509641
- Bunker, A.J., Stanway, E.R., Ellis, R.S., McMahan, R.G. 2004, *MNRAS*, 355, 374
- Chapman, S.C., Scott, D., Steidel, C.C., Borys, C., Halpern, M., Morris, S.L., Adelberger, K.L., Dickinson, M., Giavalisco, M., & Pettini, M. 2000, *MNRAS*, 319, 318
- Chapman, S.C., Blain, A.W., Smail, I., & Ivison, R.J. 2005, *ApJ*, 622, 772
- Connolly, A.J., Szalay, A.S., Dickinson, M., SubbaRao, M.U., & Brunner, R.J. 1997, *ApJ*, 486, L11
- Cowie, L.L., Songaila, A., Hu, E.M., & Cohen, J.G. 1996, *AJ*, 112, 839
- Eales, S., et al. 1999, *ApJ*, 515, 518
- Ferguson, H.C., Dickinson, M., & Williams, R. 2000, *ARA&A*, 38, 667
- Ferguson, H.C., Dickinson, M., & Papovich, C. 2002, *ApJ*, 569, L65
- Fernández-Soto, A., Lanzetta, K.M., & Chen, H.-W. 2003, *MNRAS*, 342, 1215
- Gabasch, A. et al. 2004a, *A&A*, 421, 41
- Gabasch, A. et al. 2004b, *ApJ*, 616, L83
- Giavalisco, M. et al. 2004a, *ApJ*, 600, L93
- Giavalisco, M. et al. 2004b, *ApJ*, 600, L103
- Gnedin, N.Y. & Ostriker, J.P. 1997, *ApJ*, 486, 581
- Hall, P.B., Sawicki, M., Martini, P., Finn, R.A., Pritchett, C.J., Osmer, P.S., McCarthy, D.W., Evans, A.S., Lin, H., & Hartwick, F.D.A. 2001, *AJ*, 121, 1840
- Heckman, T.M., Sembach, K.R., Meurer, G.R., Leitherer, C., Calzettin, D., & Martin, C.L. 2001, *ApJ*, 558, 56
- Inoue, A.K., Iwata, I., Deharveng, J.-M., Buat, V., & Burgarella, D. 2005, *A&A*, 435, 471
- Iwata, I., Ohta, K., Tamura, N., Ando, M., Wada, S., Watanabe, C., Akiyama, M., & Aoki, K. 2003, *PASJ*, 54, 415
- Iwata, I., Inoue, A.K., & Burgarella, D. 2005, *A&A*, 440, 881
- Iwata, I., Ohta, K., Ando, M., Kiuchi, G., Tamura, N., Akiyama, M., & Aoki, K. 2006a, astro-ph/0510829
- Iwata, I., et al. 2006b, in preparation
- Kennicutt Jr., R.C., 1998, *ARA&A*, 36, 189
- Lehnert, M.D., Bremer, M.N. 2003, *ApJ*, 593, 630
- Leitherer, C., Schaerer, D., Goldader, J.D., González Delgado, R.M., Robert, C., Kune, D.F., de Mello, D.F., Devost, D., Heckman, T. 1999, *ApJS*, 123, 3
- Lilly, S.J., Le Fèvre, O., Hammer, F., & Crampton, D. 1996, *ApJ*, 460, L1
- Madau, P. 1995, *ApJ*, 441, 18
- Madau, P., Ferguson, H.C., Dickinson, M.E., Giavalisco, M., Steidel, C.C., & Fruchter, A. 1996, *MNRAS*, 283, 1388
- Madau, P., Pozetti, L., & Dickinson, M. 1998, *ApJ*, 498, 106
- Madau, P., Haardt, F., & Rees, M.J. 1999, *ApJ*, 514, 648
- Martin, C.L. & Sawicki, M. 2004, *ApJ*, 603, 414
- Meiksin, A. 2005, *MNRAS*, 356, 596
- Miralda-Escudé, J. 2003, *ApJ*, 597, 66
- Furlanetto, S.R. & Oh, S.P. 2005, *MNRAS*, 363, 1031
- Oke, J.B., 1974, *ApJS*, 236, 27
- Ouchi, M., et al. 2004, *ApJ*, 611, 660
- Papovich, C., Dickinson, M., & Ferguson, H.C. 2001, *ApJ*, 559, 620
- Pérez-González, P.G., Zamorano, J., Gallego, J., Aragón-Salamanca, A., Gil de Paz, A. 2003, *ApJ*, 591, 827
- Pérez-González, P.G. et al. 2005, *ApJ*, 630, 82
- Press, W.H., Flannery, B.P., Teukolsky, S.A., & Vetterling, W.T. 1986, *Numerical Recipes* (Cambridge: Cambridge University Press)
- Reddy, N.A. & Steidel, C.C. 2004, *ApJ*, 603, L13
- Reddy, N.A., Erb, D.K., Steidel, C.C., Shapley, A.E., Adelberger, K.L., & Pettini, M. 2005, *ApJ*, 633, 748
- Salpeter, E.E. 1955, *ApJ*, 121, 161
- Sawicki, M.J., Lin, H., & Yee, H.K.C. 1997, *AJ*, 113, 1
- Sawicki, M. & Yee, H.K.C. 1998, *AJ*, 115, 1329
- Sawicki, M. 2001, *AJ*, 121, 2405
- Sawicki, M., Stevenson, M., Barrientos, L.F., Gladman, B., Mallén-Ornelas, G., & van den Bergh, S. 2005, *ApJ*, 627, 621
- Sawicki, M. & Thompson, D. 2005, *ApJ*, 635, 100 (KDF I)
- Sawicki, M. & Thompson, D. 2006, *ApJ*, 642, 653, (KDF II)
- Sawicki, M. & Webb, T.M.A. 2005, *ApJ*, 618, L67
- Sawicki, M. et al. 2006, in prep.
- Schechter, P. 1976, *ApJ*, 203, 297
- Schiminovich, D., et al. 2005, *ApJ*, 619, L47
- Shapley, A.E., Steidel, C.C., Adelberger, K.L., & Pettini, M. 2001, *ApJ*, 562, 95
- Shapley, A.E., Steidel, C.C., Erb, D.K., Reddy, N.A., Adelberger, K.L., Pettini, M., Barmby, P., & Huang, J. 2005, *ApJ*, 626, 698
- Smail, I., Ivison, R.J., & Blain, A.W. 1997, *ApJ*, 490, L5
- Steidel, C.C., Adelberger, K.L., Giavalisco, M., Dickinson, M., & Pettini, M. 1999, *ApJ*, 519, 1
- Steidel, C.C., Pettini, M., & Adelberger, K.L. 2001, *ApJ*, 546, 665
- Steidel, C.C., Adelberger, K.L., Shapley, A.E., Pettini, M., Dickinson, M., & Giavalisco, M. 2003, *ApJ*, 592, 728
- Steidel, C.C., Shapley, A.E., Pettini, M., Adelberger, K.L., Erb, D.K., Reddy, N.A., & Hunt, M.P. 2004, *ApJ*, 604, 534
- Stiavelli, M., Fall, S.M., & Panagia, N. 2004, *ApJ*, 610, L1
- Tresse, L., Maddox, S.J., Le Fèvre, O., & Cuby, J.-G. 2002, *MNRAS*, 337, 369
- Vijh, U., Witt, A.N., & Gordon, K.D. 2003, *ApJ*, 587, 533
- Webb, T.M.A., Eales, S., Foucaud, S., Lilly, S. J., McCracken, H., Adelberger, K., Steidel, C., Shapley, A., Clements, D. L., Dunne, L., Le Fèvre, O., Brodwin, M., Gear, W. 2003, *ApJ*, 582, 6
- Williams, R.J., et al. 1996, *AJ*, 112, 1335
- Willott, C.J., Delfosse, X., Forveille, T., Delorme, P., & Gwyn, S. 2005, *ApJ*, 633, 630
- Wyder, T.K., et al. 2005, *ApJ*, 619, L15
- Yan, H. & Windhorst, R.A. 2004, *ApJ*, 600, L1

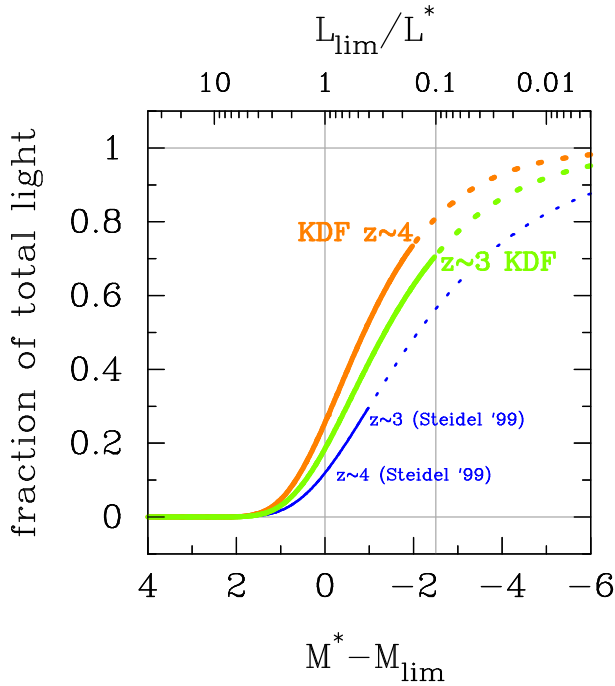


FIG. 1.— The amount of total light above a limiting magnitude  $M_{lim}$  in a Schechter function with faint end slope  $\alpha$ . The colored lines represent our KDF results at  $z \sim 3$  (green) and  $z \sim 4$  (orange) and the ground-based  $z \sim 3$  and  $z \sim 4$  surveys of Steidel et al. (1999; blue). The solid parts of these lines show the directly observed galaxies (down to the respective limiting depths of these surveys) and the dashed lines illustrate extrapolations below the completeness limits. The Steidel et al. (1999) ground-based work detects only  $\sim 1/3$  of the UV light at  $z \sim 3$  (and even less at  $z \sim 4$ ), while the KDF captures  $\sim 75\%$  of the UV light at these redshifts.

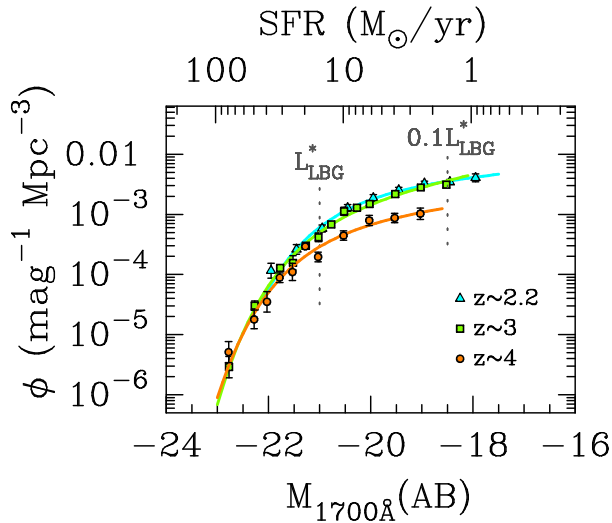


FIG. 2.— The luminosity functions of UV-selected star-forming galaxies at  $z \sim 4$ , 3, and 2.2 derived by Sawicki & Thompson (2006). The  $z \sim 4$  and  $z \sim 3$  LFs are very robust against systematic effects; at  $z \sim 2.2$ , the number density of galaxies is *not less* than that shown and if it is higher than shown, then it is so by no more than a factor of  $\sim 2$ .

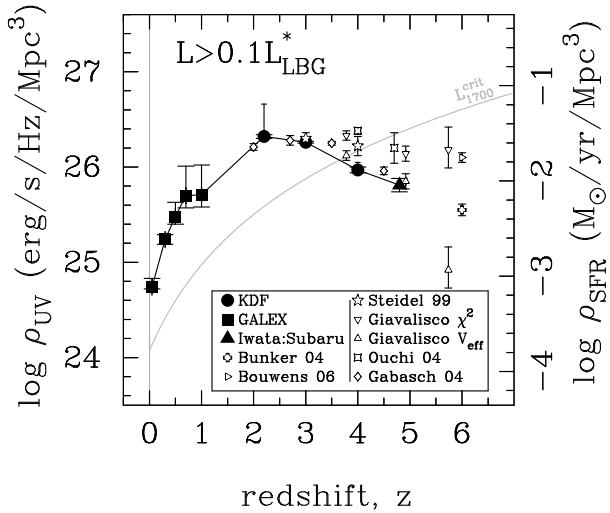


FIG. 3.— The UV luminosity density in galaxies brighter than  $0.1L_{LBG}^*$ . Solid symbols show values from the present KDF work at  $z \sim 2$ ,  $z \sim 3$ , and  $z \sim 4$ , from GALEX (at  $z \leq 1$ ) and from Iwata et al. (2006;  $z \sim 5$ ). Also shown are results from other recent work. Two errorbars are shown for the KDF points: the (generally smaller) errorbars with long terminals include both Poisson statistics and a bootstrap-resampling estimate of cosmic variance (many of the other surveys show Poisson errorbars only); the (generally larger) errorbars, most prominent at  $z \sim 2$ , include an estimate of the *maximum* possible systematic error effect in our modelling of the survey volume (see Sawicki & Thompson 2006 for details). The star formation rate density (right axis) is calculated from the UV luminosity density without correction for dust. The curve labelled  $L_{1700}^{crit}$  shows the amount of 1700Å light expected — on the basis of the calculation in § 4.3 — to be needed if starforming galaxies are to maintain ionization of the intergalactic gas.

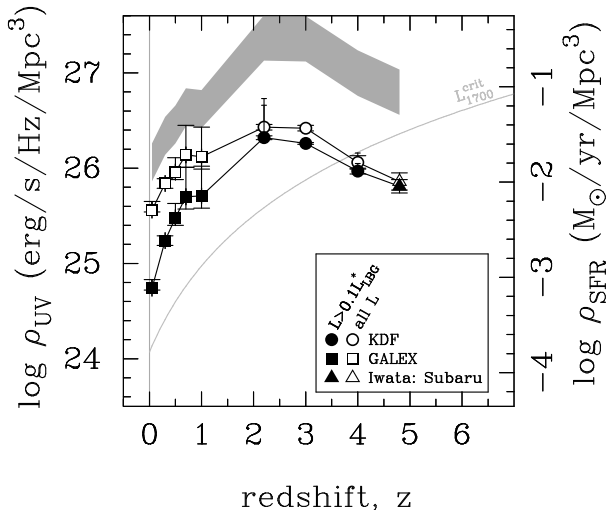


FIG. 4.— The *total* luminosity density and dust corrections. Filled symbols show the luminosity density due to galaxies brighter than  $L_{LBG}^*$ , while open symbols show the total (all  $L$ ) luminosity density. The gray band shows the range after the light from the total (all  $L$ ) UV-bright galaxy population has been corrected for dust obscuration as discussed in § 3.2.

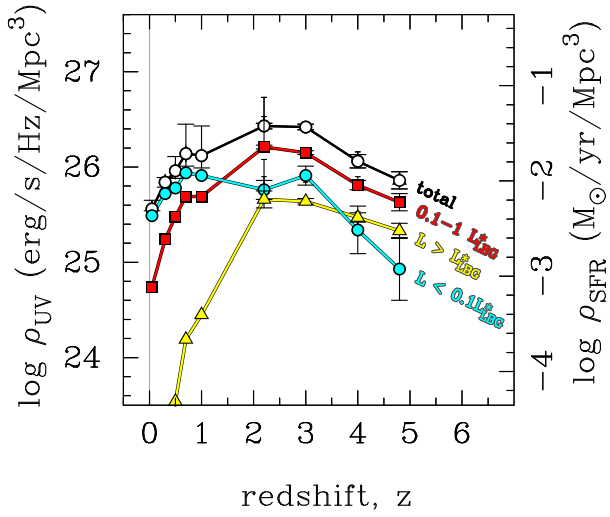


FIG. 5.— Contributions of galaxies with different individual luminosities to the total UV luminosity density of the Universe. Open circles show the total luminosity density while colored symbols show the luminosity density split by galaxy luminosity. The split is at  $L_{LBG}^*$  and  $0.1L_{LBG}^*$  (i.e.,  $M_{1700} = -21.0$  and  $-18.5$ , respectively). Galaxies with  $L = 0.1-1L_{LBG}^*$  (red squares) dominate the total luminosity density at high redshift, while those fainter than  $0.1L_{LBG}^*$  take over at  $z \lesssim 1$ . At no redshift are galaxies brighter than  $L_{LBG}^*$  dominant.

TABLE 1. REST-FRAME 1700Å UV LUMINOSITY DENSITIES<sup>a</sup>

$z$	total	$L > L_{LBG}^*$	$1 > L/L_{LBG}^* > 0.1$	$L < 0.1L_{LBG}^*$	survey
0.05	$25.56^{+0.08}_{-0.08}$	$18.56^{+8.45}_{-8.45}$	$24.74^{+0.14}_{-0.14}$	$25.49^{+0.08}_{-0.08}$	GALEX
0.3	$25.84^{+0.17}_{-0.17}$	$20.73^{+4.90}_{-4.90}$	$25.24^{+0.25}_{-0.25}$	$25.72^{+0.17}_{-0.17}$	GALEX
0.5	$25.96^{+0.40}_{-0.40}$	$23.54^{+0.83}_{-0.83}$	$25.48^{+0.29}_{-0.29}$	$25.78^{+0.47}_{-0.47}$	GALEX
0.7	$26.14^{+0.56}_{-0.56}$	$24.19^{+0.81}_{-0.81}$	$25.69^{+0.32}_{-0.32}$	$25.94^{+0.66}_{-0.66}$	GALEX
1.0	$26.12^{+0.78}_{-0.78}$	$24.45^{+0.80}_{-0.80}$	$25.69^{+0.33}_{-0.33}$	$25.91^{+0.97}_{-0.97}$	GALEX
1.7	$26.75^{+0.02}_{-0.02}$	$25.59^{+0.15}_{-0.15}$	$26.63^{+0.02}_{-0.02}$	$26.03^{+0.05}_{-0.05}$	KDF
2.2	$26.43^{+0.03}_{-0.03}$	$25.66^{+0.09}_{-0.09}$	$26.21^{+0.02}_{-0.02}$	$25.76^{+0.10}_{-0.10}$	KDF
3.0	$26.42^{+0.03}_{-0.03}$	$25.64^{+0.03}_{-0.03}$	$26.15^{+0.02}_{-0.02}$	$25.91^{+0.10}_{-0.10}$	KDF
4.0	$26.06^{+0.07}_{-0.07}$	$25.47^{+0.05}_{-0.05}$	$25.81^{+0.05}_{-0.05}$	$25.34^{+0.25}_{-0.25}$	KDF
4.8	$25.86^{+0.09}_{-0.09}$	$25.33^{+0.08}_{-0.08}$	$25.63^{+0.09}_{-0.09}$	$24.93^{+0.33}_{-0.33}$	Iwata et al. (2006) <sup>b</sup>

<sup>a</sup>In logarithmic units of erg/s/Hz/Mpc<sup>3</sup><sup>b</sup>Computed by us from data kindly provided by these authors in advance of publicationTABLE 2. UV LUMINOSITY DENSITIES IN GALAXIES BRIGHTER THAN  $0.1L_{LBG}^*$ 

Survey	$z$	$\log(\rho_{UV}^a)$
GALEX	0.05	$24.74^{+0.14}_{-0.14}$
	0.3	$25.24^{+0.25}_{-0.25}$
	0.5	$25.48^{+0.29}_{-0.29}$
	0.7	$25.70^{+0.34}_{-0.34}$
	1.0	$25.71^{+0.35}_{-0.35}$
KDF	2.2	$26.32^{+0.02}_{-0.02}$
	3.0	$26.26^{+0.01}_{-0.01}$
	4.0	$25.97^{+0.03}_{-0.03}$
Iwata et al. (2006) <sup>b</sup>	4.8	$25.81^{+0.07}_{-0.07}$
Steidel et al. (1999)	3	$26.30^{+0.06}_{-0.06}$
	4	$26.22^{+0.10}_{-0.10}$
Giavalisco et al. (2004) $\chi^2$ method	3.78	$26.33^{+0.05}_{-0.05}$
	4.92	$26.14^{+0.08}_{-0.08}$
	5.74	$26.18^{+0.24}_{-0.19}$
Giavalisco et al. (2004) $V_{eff}$ method	3.78	$26.12^{+0.05}_{-0.05}$
	4.92	$25.85^{+0.08}_{-0.08}$
	5.74	$24.92^{+0.24}_{-0.19}$
Bunker et al. (2004)	6	$25.55^{+0.06}_{-0.06}$
Bouwens et al. (2006)	6	$26.10^{+0.05}_{-0.05}$
Ouchi et al. (2004)	4.0	$26.38^{+0.04}_{-0.04}$
	4.7	$26.20^{+0.16}_{-0.16}$
Gabasch et al. (2004a, 2004b)	2.0	$26.21^{+0.04}_{-0.04}$
	2.7	$26.28^{+0.05}_{-0.05}$
	3.5	$26.25^{+0.02}_{-0.02}$
	4.5	$25.96^{+0.04}_{-0.04}$

<sup>a</sup>Rest-1700Å luminosity density in units of erg/s/Hz/Mpc<sup>3</sup><sup>b</sup>Computed by us from data kindly provided by these authors in advance of publication